

Chapter 2

Emergent Feature Sensitivity in a Model of the Auditory Thalamocortical System

Martin Coath, Robert Mill, Susan L. Denham, and Thomas Wennekers

Abstract If, as is widely believed, perception is based upon the responses of neurons that are tuned to stimulus features, then precisely what features are encoded and how do neurons in the system come to be sensitive to those features? Here we show differential responses to ripple stimuli can arise through exposure to formative stimuli in a recurrently connected model of the thalamocortical system which exhibits delays, lateral and recurrent connections, and learning in the form of spike timing dependent plasticity.

2.1 Introduction

Since Hubel and Wiesel [11] showed that, for neurons in visual cortex there were ‘preferred stimuli’ which evoked a more vigorous response than all other stimuli, it has become commonplace to think of neurons, or clusters of neurons, as having stimulus preferences—or alternatively as responding to ‘features’ of the stimulus.

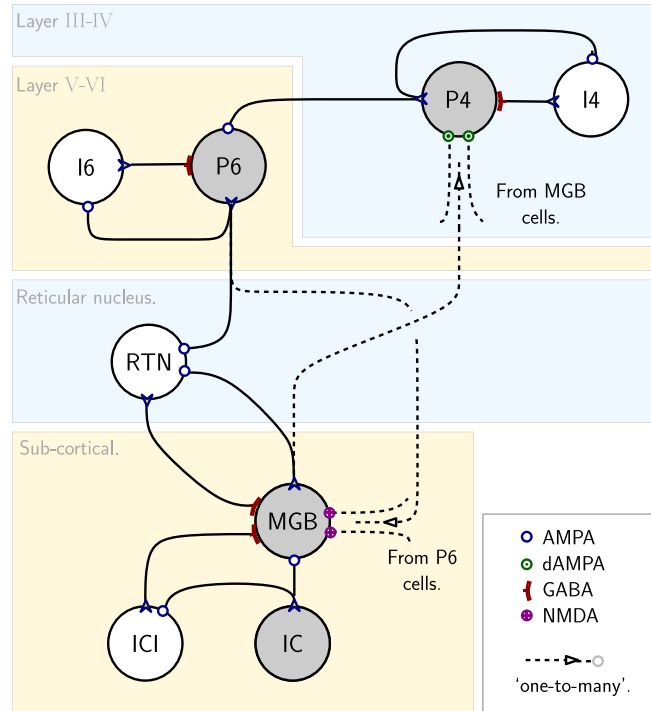
Although it is widely believed that auditory perception is based on the responses of neurons that are tuned to features of the stimulus it is not clear what these features are or how they might come in to existence. There is, however, evidence that cortical responses develop to reflect the nature of stimuli in the early post-natal period [12, 24, 25] and that this plasticity persists beyond early development [20]. In addition it has been shown that excitatory corticofugal projections to the thalamus are likely to be crucial in thalamic plasticity and hence in the representation of the stimulus that is available to the cortex [7].

The work presented here is motivated by the desire to investigate whether a recurrently connected thalamocortical model exhibiting spike time dependent plasticity (STDP) can be sensitized to specific features of a stimulus by exposure. Modelling studies have suggested [4, 5] that the spectro-temporal patterns found in a limited number of stimuli, which reflect some putative early auditory environment, may bootstrap the formation of neural responses and that unsupervised, correlation based learning leads to a range of responses with features similar to those reported from measurements *in vivo*. However in this previously reported work the model of STDP adopted, mostly for reasons of computational efficiency, was based on average activity over a period of time rather than the times of the spikes themselves. In addition this model also led to some synaptic weights increasing without limit and hence an arbitrary cut-off in the time used for training.

Here we employ a model of plasticity that depends on times of pre-synaptic spikes and a variable representing the post-synaptic activity [2] and avoids the problem of unlimited weights by using synapses that are bi-stable, that is, over time the weights of all synapses tend to one or zero. We

M. Coath (✉)
University of Plymouth, Drake Circus, PL4 8AA, UK
e-mail: mcoath@plymouth.ac.uk

Fig. 2.1 Each vertical sub-unit of the network consists of eight neurons. The sub-cortical section receives input from one stimulus channel representing a position on the tonotopic axis. Each thalamic (MGB) cell is connected to a number of cortical cells representing layer IV, the principal receiving layer. Layer VI cells recurrently connect the cortex to the thalamus *via* NMDA synapses which exhibit STDP and thus are the loci of the correlation-based learning in the network



show that a model of auditory cortex incorporating lateral spread of excitation with associated delays, recurrent connections between layers, and exhibiting STDP (learning) adapts during exposure to training patterns (stimuli) in a way that is determined partly by the stimuli themselves, and the resulting network exhibits ‘feature preferences’ that could support the representation of the input in a high dimensional feature space.

2.2 Methods

2.2.1 The Network

2.2.1.1 Network Architecture

The model auditory cortex consists of five hundred repeating units each consisting of eight neurons arranged in layers, as illustrated in Fig. 2.1. The lower, sub-cortical, section represents the junction of the inferior-colliculus (IC) with the medial geniculate body of the thalamus (MGB). The upper section represents a two-layer cortical structure consisting of a receiving layer (layer IV [22] marked simply as P₄ in Fig. 2.1) and a second layer (marked as P₆ in the figure) providing a recurrent excitatory connection to the thalamus [10], and recurrent inhibitory connection to the thalamus via the thalamic reticular nucleus (RTN) [9, 10]. Inhibitory inputs to the thalamus also come from the IC, in this case via a GABA-type interneuron, although there is evidence for direct connections from GABAergic cells in IC [14, 21].

The recurrent excitatory connections from P₆ to MGB are mediated by NMDA type synapses that are the loci of the STDP (see Sect. 2.2.2). This approach reflects the belief that the principle role of such corticofugal connections is to modulate thalamocortical transmission and that “corticofugal

modulation is an important mechanism for learning induced or experience-dependent auditory plasticity” [17, 26]. Although it is clear that some of the changes associated with this plasticity must be located in the cortex, there is recent evidence that corticothalamic synapses are regulated by cortical activity during the early developmental period [23].

2.2.1.2 Neurons

The neurons used are linear integrate-and-fire units and use a stimulation paradigm not of current injection, but of conductance injection which moves integrate-and-fire models closer to a situation that cortical neurons would experience in vivo [6]. This modification also allows the use of conductance-based synapses as described in Sect. 2.2.1.3 below.

The behaviour of the neurons can be described by:

$$\tau \frac{dV}{dt} = -(V(t) - E_L) - \sum_i w_i \cdot (V(t) - E_{Ri})$$

$$\text{if } V > V_T \quad \text{then } V \rightarrow E_L : Z(t) \rightarrow 1 \text{ else } Z(t) \rightarrow 0 \quad (2.1)$$

where τ is the membrane time constant, V the membrane potential, $E_L = 0$ the leak reversal potential, $w_i(t)$ is the weight of the i th synapse—this is a function of time because the value of w subsumes not only the weight constant but also the time varying conductance of the synapse (see Sect. 2.2.1.3), $V_T = 1$ is the firing threshold potential, and $Z(t)$ is the output of the neuron expressed as delta functions at firing times. Values for τ were assigned identically and independently randomly from an equal distribution (i.i.d.) in the range 9–11 ms. The value E_{Ri} is the reversal potential of the i th synapse.

In addition all neurons received i.i.d. current injections representing the sum of non-stimulus-specific activity. This has the effect of bringing the neurons closer to threshold and the range of values was chosen such that a low level (<1 Hz) of spontaneous action potentials was evoked.

2.2.1.3 Synapses

There are four types of synapse present in the model. Each exhibits a time dependent conductance which is derived from the train of spikes (delta functions) originating in the pre-synaptic neuron. The conductance is the output of a second-order low-pass filter and the resulting temporal response function for a single spike is an alpha-function characterised by two parameters: the rise-time τ_r and the decay-time τ_d .

The majority of excitatory synapses have fast rise and fall times and are designated AMPA types. Other excitatory synapses in the thalamocortical projections have longer rise and fall times and are designated as NMDA synapses. Inhibitory synapses are all of the same type which have very fast rise times and intermediate fall time and these are designated as GABA. The time constants are given in Table 2.1 [8].

Table 2.1 Time constants used in synapse models

	τ_r	τ_d
AMPA	0.90 ms	1.50 ms
GABA	0.01 ms	5.00 ms
NMDA	3.00 ms	40.00 ms

2.2.1.4 Depressing Synapses

The axons that project from MGB to layer IV of the cortex have the same time constants as other AMPA synapses but exhibit synaptic depression and are referred to as dAMPA. The dynamical properties of cortical synapses can influence the temporal sensitivity of cortical circuitry. Here we use a model of synaptic depression which is characterised by the variable representing the running fraction of available neurotransmitter $x(t)$ that recovers to unity with a time constant τ_A [19].

$$\frac{dx}{dt} = \frac{1-x}{\tau_A} - x \cdot Z(t) \quad (2.2)$$

The time constant τ_A was adjusted so as to be consistent with paired pulse ratios reported in in vivo studies of pyramidal neurons [1]. All simulations were run with $\tau_A = 30$ ms.

2.2.1.5 Connections Between Columns

The excitatory afferents from the thalamus to each cell in the cortical receiving layer come from a number of MGB cells as indicated in Fig. 2.1. These are selected based on connection probabilities that vary with the distance between cells as shown in (2.3), i.e. falling as the inter-column distance d increases. The maximum probability of a connection being made is at $d = 0$ and this value is controlled by the variable C and the ‘width’ of the function is determined by s . All simulations were run with $C = 0.2$, $s = 20$.

In a similar way the corticothalamic connections to each MGB cell also come from a number of P_6 cells selected in a similar way. For these connections $C = 0.1$, $s = 100$. The probability of connection is given by:

$$P = C \cdot \exp\left(\frac{-0.5 \cdot d^2}{s^2}\right) \quad (2.3)$$

For each of the 500,000 possible connections in the cortico-thalamic and thalamocortical projections a Boolean value was chosen with the probability of TRUE being P and a synapse created, or not, accordingly.

These ‘fan out’ connections give the opportunity for cortical neurons to integrate information from heterotopic areas of thalamus and also stand as surrogates for the cortico–cortical connections [18] which have no explicit representation in this model. The cortico–thalamic connections are mediated via NMDA type synapses which are the loci of the STDP and hence the correlation-based learning in the network, see Sect. 2.2.2.

2.2.1.6 Delays

In order to investigate the role played by the temporal structure of the stimuli in the emergent stimulus preferences of the network, delays were incorporated in to the network. Assumptions were made about the dimensions of the cortical area represented by the model and the range of values for axonal propagation rates. Using these two figures, distance dependent delays were introduced for fan-out connections in the model based on the inter-column distance.

Under the simplifying assumption that the delay increases linearly with d we have assumed a maximum separation between neurons of 1 cm and values of axonal propagation rate from 0.5 – 10.0 ms^{-1} .

2.2.2 Synaptic Plasticity

Spike-timing-dependent plasticity (STDP) is the modification of synaptic weights based on the correlation between pre- and post-synaptic firing times. Evidence for this has been gathered in vitro, and is beginning to emerge in vivo [13], and it is believed to be a feature of synapses which have NMDA receptors that regulate the genes required for long term maintenance of these changes [15]. In general, if a pre-synaptic spike precedes a post-synaptic spike then the synapse is potentiated; if the timing of the spikes is reversed then the synapse is depressed.

One problem with correlation-based learning is that the weight changes are unstable and additional mechanisms have to be invoked to ensure that weights do not increase in an uncontrolled manner. Our approach in earlier work was to start with very low weights and keep the training short [3]. In this way we see how the pattern of weight changes establishes itself in the early stages of training. Another possibility, the approach that is adopted here, is to implement a form of STDP in which the weights are bi-stable [2].

The learning rule used in the results presented here is summarized in (2.4), (2.5), and (2.6). At the arrival time of each pre-synaptic spike the synaptic efficacy X is modified based on the post-synaptic neuron membrane potential V and the post-synaptic neuron internal state variable C . The variable C is identified with the calcium concentration [16] and is determined by a leaky integration of post-synaptic spiking activity with a relatively slow time constant τC :

$$\frac{dC(t)}{dt} = -\frac{1}{\tau_C}C(t) + J_C \sum_i \delta(t - t_i) \quad (2.4)$$

where J_C is the contribution of a single post-synaptic spike. The synapse is potentiated by a small amount a if V is above a pre-determined threshold θ_V and C is within set limits θ_{up}^l and θ_{up}^h . Similarly the synapse is de-potentiated by an amount b if V is less than or equal to θ_V and C is within a different pair of bounds θ_{down}^l and θ_{down}^h :

$$\begin{aligned} X &\rightarrow X + a & \text{if } V(t_{pre}) > \theta_V & \text{ and } \theta_{up}^l < C(t_{pre}) < \theta_{up}^h \\ X &\rightarrow X - b & \text{if } V(t_{pre}) \leq \theta_V & \text{ and } \theta_{down}^l < C(t_{pre}) < \theta_{down}^h \end{aligned} \quad (2.5)$$

If no modification is triggered by the conditions in (2.5) (including in the absence of pre-synaptic spikes) X drifts towards one of two stable states depending on whether it is greater than a threshold value θ_X :

$$\begin{aligned} \frac{dX}{dt} &= \alpha & \text{if } X > \theta_X \\ \frac{dX}{dt} &= -\beta & \text{if } X \leq \theta_X \end{aligned} \quad (2.6)$$

where α and β are positive constants.

2.2.3 Training

Each of the stimuli used in these experiments consists of a pattern of current injection into the units representing neurons of the inferior colliculus, these are marked IC in Fig. 2.1. Although, for simplicity, these patterns of current injection are not derived from audio files via a cochlear model they can be thought of as time varying patterns of activity across the tonotopic axis represented by the one dimensional array of IC cells.

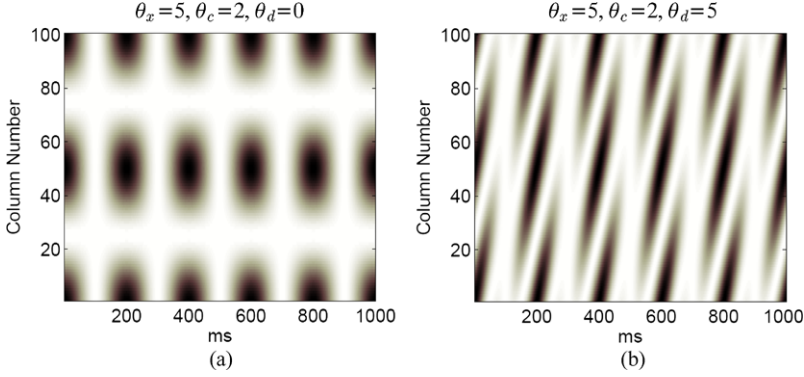


Fig. 2.2 Example stimuli used in training the network. Each example, in common with all such stimuli used in the experiments, have a 5 Hz amplitude modulation rate. **(a)** A stimulus with no FM component, and **(b)** a stimulus with a slowly moving up FM component (determined by θ_d). In the work reported here stimuli varied only in the value for θ_d

2.2.3.1 Parametric AM/FM Stimuli

The stimuli were all of the form given by (2.7) below:

$$z(t, c) = \frac{(\cos(2\pi t\theta_x) + 1)(\cos(2\pi(c\theta_c + t\theta_d) + 1))}{4} \quad (2.7)$$

where $z(t, c)$ is the value of the current injection at time t and in channel c .

The parameters θ_x , θ_c and θ_d can be adjusted to give sweeps or gratings that move in the tonotopic axis with time, and also patches of stimulation that have a temporal amplitude modulation (AM) but no frequency modulation (FM) component. Examples of such stimuli are shown below in Fig. 2.2.

The value of θ_x , the temporal modulation rate, was fixed at 5 for all experiments. This value was chosen because of the inherent low-pass nature of the thalamocortical projections caused by the depressing synapses, (see Fig. 2.1) hence stimuli with temporal modulation rates much greater than 5 would drive the cortical receiving layer only weakly. In addition rates of temporal modulation around 4–5 Hz are important for communication signals such as the syllable rate for human speech. The value of θ_c , the spectral density, was fixed at 2.

For each experiment one value of θ_d was chosen as the training stimulus. The network was then exposed to 50 epochs (each 2 seconds) of this stimulus with the learning rule turned on. Between each of these learning phases the response of the network was recorded to 10 other stimuli. These are referred to as test stimuli, with a range of values for θ_d both positive and negative. Each test and training stimulus was separated from the previous one by ≈ 300 ms of random current injection at the same mean level as the stimuli and the phase of the stimulus advanced by a random value from 0 to 2π to ensure that both the training and test stimuli were not presented starting at the same phase in all cases, this process is summarised in Fig. 2.3. In the results section we consider networks trained with the values for θ_d of -10 , -5 , 0 , 5 , 10 . Fixing θ_d at integer multiples of θ_x produces stimuli with similar temporal characteristics in that the maxima of the current injections occur in the same channels with each presentation.

2.2.3.2 Random Chord Stimuli

We also consider results of training with stimuli that consist of injections of current in channels chosen at random ($P = 0.1$) for short periods of time chosen from an equal distribution from 20–60 ms. These noise-like ‘random chord’ stimuli are more suitable than random current injections representing white noise which drive the cortical receiving layer only very weakly.

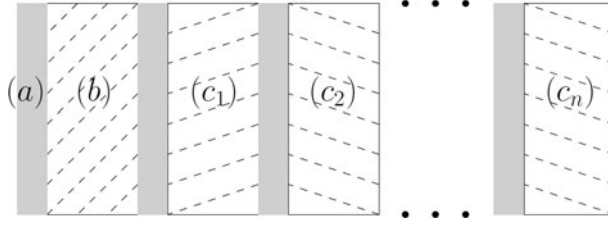
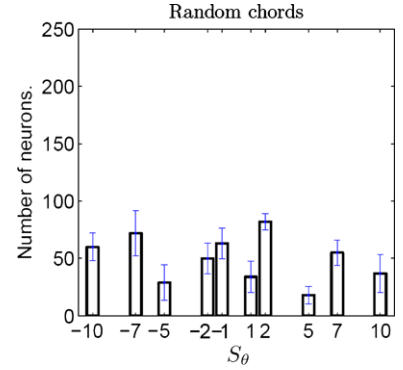


Fig. 2.3 One epoch of the training process. The sequence consists of (a) noise; before every stimulus there was 300 ms of random current injection at a mean level the same as the stimuli, (b) training; one value of θ_d was chosen as the FM component of the training stimulus, (c_1, \dots, c_n) testing; the response of the network was recorded during 10 test stimuli with different values of θ with the learning rule switched off. Each experiment consisted of 30 of these epochs

Fig. 2.4 The distribution of the directional sensitivity (S_θ , see (2.8)) after training with ‘noise like’ random chord stimulus. The results obtained after 30 epochs (see Fig. 2.3) show no clear sensitivity to any preferred FM sweep rate



2.3 Results

Of interest are both the responses of the network and the responses of the individual neurons. In both cases the questions are: (a) what, if any, aspect of the stimulus is the individual neuron or network of neurons sensitive to after training and (b) is the distribution of sensitivities different for different training stimuli. In the results presented here the responses were measured in the thalamic (MGB) section of the network as this is the locus of plasticity in the current study and we will consider results using the five training stimuli i.e. $\theta_d = -10, -7, -5, -0, 5, 7, 10$. We will also consider results from training with random chord stimuli (see Sect. 2.2.3).

To help us describe the results we can define the direction sensitivity S of a neuron as the log ratio of the spike count R at any given θ for up and down versions of the stimulus.

$$S = \log \frac{R_{\theta_{\max}}}{R_{\theta_{\min}}} \quad (2.8)$$

The value of θ which gives the maximum absolute value of S is the rate of change to which the neuron is most sensitive which we will indicate as S_θ . Because the highest spike count is always in the numerator of (2.8) we append the sign representing the direction which gives the highest spike count to indicate the preferred direction.

The first experiment was to determine the stimulus preferences of the MGB neurons in the case where the training stimulus consists of random chords. The resulting directional sensitivities are shown in Fig. 2.4. As can be seen in Fig. 2.4 there are neurons exhibiting all directional sensitivities but no clear pattern emerges during training.

The network was then exposed to stimuli having no FM component that is with $\theta_d = 0$. Figure 2.5(a) shows the spike count for each test stimulus at each training epoch and Fig. 2.5(b) shows the resulting

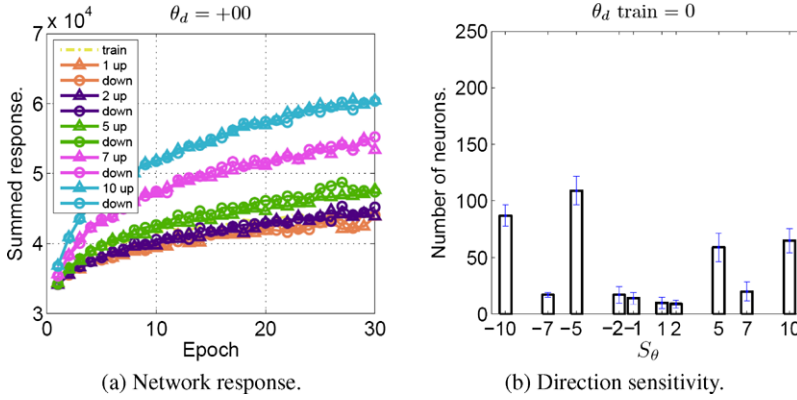


Fig. 2.5 Training with stimulus $\theta_d = 0$. (a) The summed spike count for the whole network for each of the ten test stimuli over the training period, and (b) the resulting distribution of directional sensitivities among individual MGB cells. No error bars are shown in (a) as this illustrates a single example training. Note that symbols representing up and down stimuli for all θ are superimposed indicating no overall direction preference

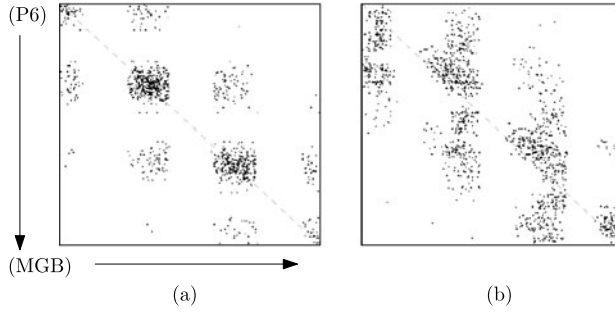


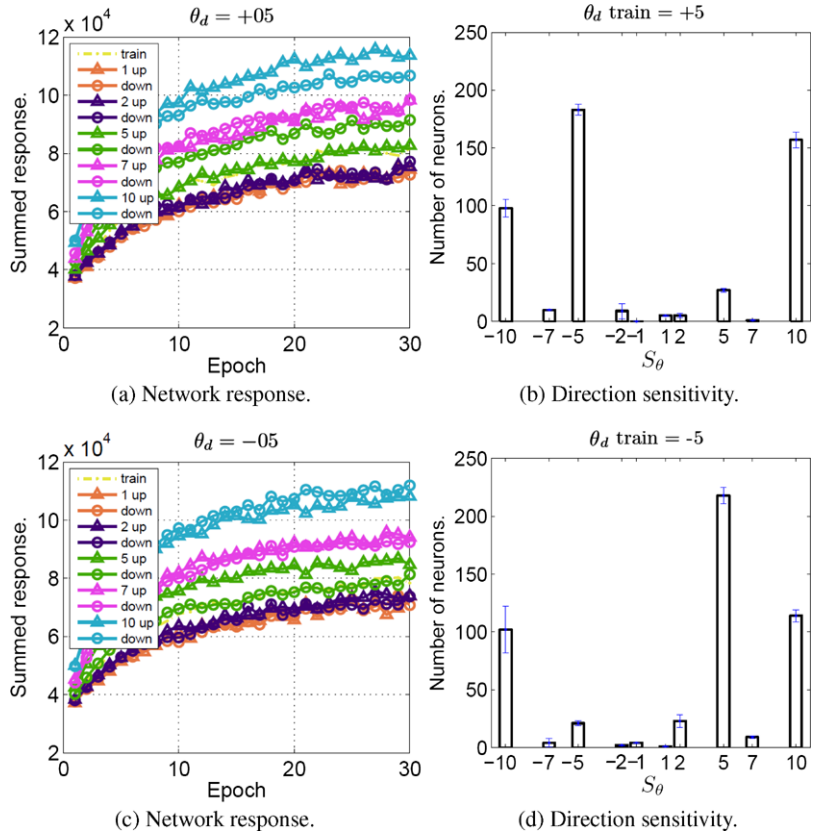
Fig. 2.6 Weights of NMDA synapses after training with (a) stimuli with $\theta_d = 0$ (no FM component) and (b) with $\theta_d = +5$. The *dotted diagonal* indicates connections between cortical and thalamic cells at the same position in the tonotopic axis. In the case of training with $\theta_d = -5$ (not shown) a pattern similar to (b) emerges but as a mirror image reflected in the *dotted diagonal*

distribution of values for S_θ . The response of the network shows no *overall* sensitivity to direction of frequency modulation, although Fig. 2.5(c) shows that there are direction sensitive neurons in the MGB after training and that these are predominantly at $\theta = \pm 5$ and $\theta = \pm 10$.

In the previous section the training stimuli had no FM component but patterns with a range of values for θ_d were used as test stimuli. In the next set of experiments the same test stimuli were used but stimuli with a single value for θ_d were used for training.

To illustrate the influence of the FM component of the stimulus on the pattern of weights Fig. 2.6 shows the pattern of corticothalamic projection weights in the NMDA synapses after exposure to stimuli with and without FM components. The nature of the learning rule is such that the overwhelming majority of synapses will have connection weights of either one or zero so the patterns of weights can be thought of as a connectivity matrix. It can be seen that the emergent connectivity for the stimulus without FM component, Fig. 2.6(a), is symmetrical around the diagonal indicated with a dashed line. Points on this diagonal represent connections between cortical cells and MGB cells at the same position on the tonotopic axis, that is with a column separation $d = 0$ see (2.3). In contrast, the connectivity pattern that emerges after training using a stimulus with FM component, Fig. 2.6(b), exhibits an asymmetry about this same diagonal. In the case illustrated the FM component used in training was

Fig. 2.7 Training with stimulus $\theta_d = \pm 5$. (a) and (c) the summed spike count for the whole network for each of the ten test stimuli over an example training period. A small difference in the network response to up and down stimuli is evident at $\theta = \pm 5$ and $\theta = \pm 10$. (b) and (d) the resulting distribution of directional sensitivities among individual MGB cells



‘up’ and in the case where the equivalent ‘down’ stimulus was used the pattern was the mirror image (not shown).

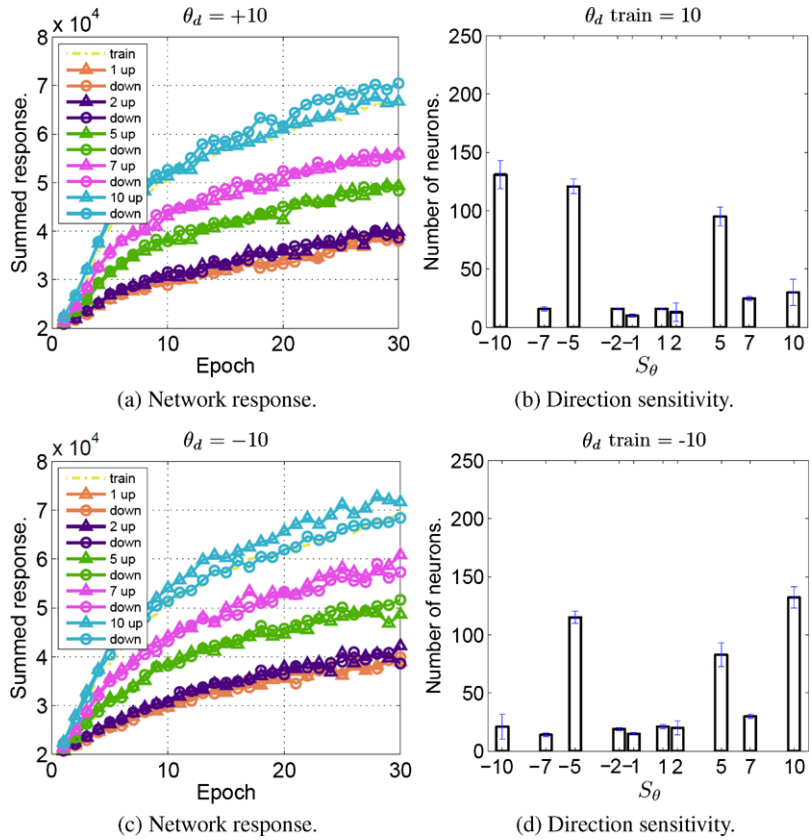
Figure 2.7 shows two results corresponding to Fig. 2.5 but after training with stimuli having $\theta_d = \pm 5$. An asymmetry emerges in the response of the whole network and this can be seen in the distribution of responses in the individual neurons. The network trained with *up* stimuli exhibits a majority of neurons with a greater sensitivity for *down* stimuli but only at $\theta = 5$, however, the emergent preference for *up* stimuli is visible for $\theta = 10$. This apparent contradiction might be due to elevated firing rates in the first few milliseconds of the preferred stimulus causing the thalamocortical synapses to depress, thus lowering the overall spike count for the training stimulus. Work is underway to confirm this hypothesis.

A corresponding result can be seen in Fig. 2.8 for training with stimuli $\theta = \pm 10$ which shows a pattern consistent with the interpretation of Fig. 2.7. Few neurons show directional sensitivity for the training stimulus but there is an increase in those with maximal directional sensitivity in the opposite direction, and in the same direction for twice the FM rate.

2.4 Discussion

The functional organization of the auditory system can be altered *in vivo* by repeated stimulation (e.g. [26]) and it has also been shown in studies of the visual system [23] that activity-dependent plasticity in cortico-thalamic connections operate during early developmental stages. The work presented here

Fig. 2.8 Training with stimulus $\theta_d = \pm 10$. (a) and (c) the summed spike count for the whole network for each of the ten test stimuli over an example training period. A small difference in the network response to up and down stimuli is evident at $\theta = \pm 10$. (b) and (d) the resulting distribution of directional sensitivities among individual MGB cells



represents the first attempt to model this sort of developmental plasticity in a biophysically motivated artificial network of spiking units.

The results show that STDP allows the model which exhibits lateral connectivity and recurrent connections to adapt to the stimuli to which they are exposed. This adaptation can, we have shown, exploit a range of axonal delays in order to represent correlations in activity at different times along a spatially defined axis such as the tonotopic axis reported in primary auditory cortex. In this way sensitivity to spectrotemporal features can emerge through exposure to stimuli both in individual neurons and neuronal ensembles.

The results provide a model which may help us understand how efferent cortical pathways to thalamic nuclei might be crucial in the development of the auditory and other sensory systems, and also how these might support other forms of plasticity such as attentional, or task-related modulation of thalamocortical transmission.

Acknowledgements This work is funded by EU FP7-ICT-231168 SCANDLE, and EPSRC EP/C010841/1 COLAMN.

References

1. Atzori, M., Lei, S., Evans, D.I., Kanold, P.O., Phillips-Tansey, E., McIntyre, O., McBain, C.J.: Differential synaptic processing separates stationary from transient inputs to the auditory cortex. *Nat. Neurosci.* **4**(12), 1230–1237 (2001). doi:[10.1038/nn760](https://doi.org/10.1038/nn760)

2. Brader, J.M., Senn, W., Fusi, S.: Learning real-world stimuli in a neural network with spike-driven synaptic dynamics. *Neural Comput.* **19**(11), 2881–2912 (2007). doi:[10.1162/neco.2007.19.11.2881](https://doi.org/10.1162/neco.2007.19.11.2881)
3. Coath, M., Balaguer-Ballester, E., Denham, S.L., Denham, M.: The linearity of emergent spectro-temporal receptive fields in a model of auditory cortex. *Biosystems* **94**(1–2), 60–67 (2008). doi:[10.1016/j.biosystems.2008.05.011](https://doi.org/10.1016/j.biosystems.2008.05.011)
4. Coath, M., Brader, J.M., Fusi, S., Denham, S.L.: Multiple views of the response of an ensemble of spectro-temporal features support concurrent classification of utterance, prosody, sex and speaker identity. *Network* **16**(2–3), 285–300 (2005)
5. Coath, M., Denham, S.L.: Robust sound classification through the representation of similarity using response fields derived from stimuli during early experience. *Biol. Cybern.* **93**(1), 22–30 (2005). doi:[10.1007/s00422-005-0560-4](https://doi.org/10.1007/s00422-005-0560-4)
6. Destexhe, A., Rudolph, M., Paré, D.: The high-conductance state of neocortical neurons in vivo. *Nat. Rev., Neurosci.* **4**(9), 739–751 (2003). doi:[10.1038/nrn1198](https://doi.org/10.1038/nrn1198)
7. Egerzenzinger, E.R., Glasier, M.M., Hahn, J.O., Pons, T.P.: Cortically induced thalamic plasticity in the primate somatosensory system. *Nat. Neurosci.* **1**(3), 226–229 (1998). doi:[10.1038/673](https://doi.org/10.1038/673)
8. Gerstner, W., Kistler, M.: *Spiking Neuron Models*. Cambridge University Press, Cambridge (2002)
9. Guillery, R.W., Feig, S.L., Lozsádi, D.A.: Paying attention to the thalamic reticular nucleus. *Trends Neurosci.* **21**(1), 28–32 (1998)
10. Guillery, R.W., Sherman, S.M.: Thalamic relay functions and their role in corticocortical communication: generalizations from the visual system. *Neuron* **33**(2), 163–175 (2002)
11. Hubel, D.H., Wiesel, T.N.: Receptive fields, binocular interaction and functional architecture in the cat's visual cortex. *J. Physiol.* **160**, 106–154 (1962)
12. Illing, R.-B.: Maturation and plasticity of the central auditory system. *Acta Oto-Laryngol., Suppl.* **552**(552), 6–10 (2004)
13. Jacob, V., Brasier, D.J., Erchova, I., Feldman, D., Shulz, D.E.: Spike timing-dependent synaptic depression in the in vivo barrel cortex of the rat. *J. Neurosci.* **27**(6), 1271–1284 (2007). doi:[10.1523/JNEUROSCI.4264-06.2007](https://doi.org/10.1523/JNEUROSCI.4264-06.2007)
14. Marie, R.L.S., Stanforth, D.A., Jubelier, E.M.: Substrate for rapid feedforward inhibition of the auditory forebrain. *Brain Res.* **765**(1), 173–176 (1997)
15. Rao, V.R., Finkbeiner, S.: NMDA and AMPA receptors: old channels, new tricks. *Trends Neurosci.* **30**(6), 284–291 (2007). doi:[10.1016/j.tins.2007.03.012](https://doi.org/10.1016/j.tins.2007.03.012)
16. Shouval, H.Z., Bear, M.F., Cooper, L.N.: A unified model of MNDA receptor-dependent bidirectional synaptic plasticity. *Proc. Natl. Acad. Sci. USA* **99**(16), 10831–10836 (2002). doi:[10.1073/pnas.152343099](https://doi.org/10.1073/pnas.152343099)
17. Suga, N., Xiao, Z., Ma, X., Ji, W.: Plasticity and corticofugal modulation for hearing in adult animals. *Neuron* **36**(1), 9–18 (2002)
18. Thomson, A.M., Bannister, A.P.: Interlaminar connections in the neocortex. *Cereb. Cortex* **13**(1), 5–14 (2003)
19. Tsodyks, M.V., Markram, H.: The neural code between neocortical pyramidal neurons depends on neurotransmitter release probability. *Proc. Natl. Acad. Sci. USA* **94**(2), 719–723 (1997)
20. Wang, X.: The unexpected consequences of a noisy environment. *Trends Neurosci.* **27**(7), 364–366 (2004). doi:[10.1016/j.tins.2004.04.012](https://doi.org/10.1016/j.tins.2004.04.012)
21. Winer, J.A., Marie, R.L.S., Larue, D.T., Oliver, D.L.: GABAergic feedforward projections from the inferior colliculus to the medial geniculate body. *Proc. Natl. Acad. Sci. USA* **93**(15), 8005–8010 (1996)
22. Winer, J.A., Miller, L.M., Lee, C.C., Schreiner, C.E.: Auditory thalamo-cortical transformation: structure and function. *Trends Neurosci.* **28**(5), 255–263 (2005). doi:[10.1016/j.tins.2005.03.009](https://doi.org/10.1016/j.tins.2005.03.009)
23. Yoshida, M., Satoh, T., Nakamura, K.C., Kaneko, T., Hata, Y.: Cortical activity regulates corticothalamic synapses in dorsal lateral geniculate nucleus of rats. *Neurosci. Res.* **64**(1), 118–127 (2009). doi:[10.1016/j.neures.2009.02.002](https://doi.org/10.1016/j.neures.2009.02.002)
24. Zhang, L., Bao, S., Merzenich, M.: Persistent and specific influences of early acoustic environments on primary auditory cortex. *Nat. Neurosci.* **4**(11), 1123–1130 (2001)
25. Zhang, L.I., Bao, S., Merzenich, M.M.: Disruption of primary auditory cortex by synchronous auditory inputs during a critical period. *Proc. Natl. Acad. Sci. USA* **99**(4), 2309–2314 (2002)
26. Zhang, Y., Yan, J.: Corticothalamic feedback for sound-specific plasticity of auditory thalamic neurons elicited by tones paired with basal forebrain stimulation. *Cereb. Cortex* **18**(7), 1521–1528 (2008). doi:[10.1093/cercor/bhm188](https://doi.org/10.1093/cercor/bhm188)

From Brains to Systems

Brain-Inspired Cognitive Systems 2010

Hernández, C.; Sanz, R.; Gómez Ramirez, J.; Smith, L.S.;

Hussain, A.; Chella, A.; Aleksander, I. (Eds.)

2011, XV, 253 p. 111 illus., 53 illus. in color., Hardcover

ISBN: 978-1-4614-0163-6